Implementing Innovative Ideas in Structural Engineering and Project Management
*Edited by* Saha, S., Zhang, Y., Yazdani, S., and Singh, A.

ISBN: 978-0-9960437-1-7

# LIVE-LOAD DISTRIBUTION FACTORS AND SERVICE RESPONSE OF MISSOURI BRIDGE A7957

E. S. HERNANDEZ and J. J. MYERS

*Dept of Civil, Architectural & Environmental Engineering,*
*Missouri University of Science and Technology, Rolla, USA*

During the last years, self-consolidating concrete (SCC) has become widely accepted because of its primary benefits that include a higher construction and cost effectiveness compared to traditional concrete mixtures. Innovative materials such as high volume fly ash concrete (HVFAC) represents a significant potential to producing stronger and more durable cast-in-place (CIP) concrete elements. Bridge A7957 is the first large-scale implementation of these materials conducted by the Missouri Department of Transportation (MoDOT) in Missouri, USA. A level of 50% fly ash to cement proportion, as well as self-consolidating concrete (SCC) with two different strengths was employed in the construction of Bridge A7957. The purpose of this study was to conduct an in-situ evaluation of the precast prestressed (PC/PS) concrete members of the bridge superstructure. To attain this objective, Bridge A7957 was scheduled to be monitored at different serviceability stages. A field load test was conducted to investigate the overall bridge's response under static loads. During the live load test, the girders' vertical deflection was obtained with an automated total station (ATS). Based on measured results, the flexural lateral distribution factors were computed. The AASHTO LRFD Bridge Design Specifications were also used to compute the flexural lateral distribution factors, which were found to be conservative.

*Keywords:* Deflection, HVFAC, Self-consolidated concrete, SCC.

## 1 INTRODUCTION

Despite the benefits that come with using high strength self-consolidating concrete (HS-SCC), there are some concerns related to its structural performance related to its constituent materials and proportions. Of particular interest is the effect of using larger paste content and smaller coarse aggregate size in the mix (Myers *et al.* 2012). It is fundamental to monitor the serviceability response of full-scale infrastructure employing HS-SCC PC/PS members. As an attempt to investigate the serviceability and structural performance both short-term and long-term of Bridge A7955's PC/PS concrete members, an instrumentation program was developed and implemented. Part of the instrumentation program consisted of monitoring the deflections of the PC/PS girders during the service life by conducting several series of live load tests.

The AASHTO LRFD Bridge Design Specifications (AASHTO 2012) equations allow computing the percentage of live load applied to a bridge that is carried by each girder (these are referred to as distribution factors). Once distribution factors are estimated, a three-dimensional (3D) structural analysis is treated as one-dimensional

(1D) structural analysis by designers (Barker and Puckett 2013). A live load effect (i.e., bending moment or shear force) is multiplied by the distribution factor to obtain a design effect applied to a 1D member instead of the whole 3D structural system. The AASHTO LRFD does not propose a method to estimate how the load is distributed among the girders for in-service assessments of bridge structures. Instead, this approach proposes a methodology that conservatively estimates distribution factors used for design. Live load tests can be used to estimate the in-service lateral load distribution based on field factors that favorably or adversely affect the response of a bridge structure (Cai and Shahawy 2003). On this research, a comparison between load factors obtained from field measurements and the AASHTO LRFD method was conducted as an effort to assess some differences between both methods.

## 2 BRIDGE DESCRIPTION

Bridge A7957 is located along Highway 50 in Osage County, Missouri. The bridge is a three-span, continuous, PC/PS concrete bridge (Figure 1). The PC/PS concrete NU53 girders (Figure 1b) in each span were designed with different concrete mixtures (Hernandez et al. 2014). Girders in the first span are 30.48 m (100 ft.) long and were made of conventional concrete (MoDOT's Class A mixture) with a specified compressive strength of 55.2 MPa (8,000 psi). Girders in the second span are 36.58 m (120 ft) and were fabricated with a HS-SCC of 68.9 MPa (10,000 psi).

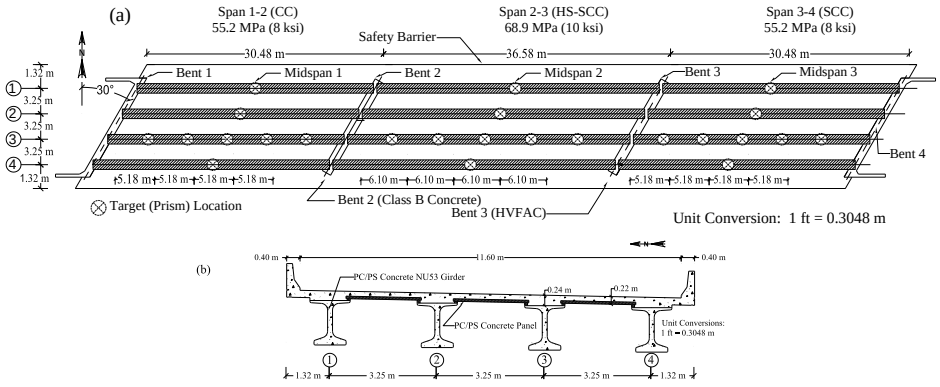


Figure 1. Bridge A7957. (a) Plan View and Prisms (ATS Targets) Locations; (b) Cross-Section.

The third span measures 30.48 m (100 ft.) and employed SCC with target compressive strength of 55.2 MPa (8,000 psi). PC/PS concrete panels, with a specified compressive strength of 41.4 MPa (6,000 psi), extend between the top flanges of the girders in the transverse direction and underneath a CIP RC deck (Figure 1b). The CIP deck was cast with a 25 % fly ash replacement of portland cement concrete mixture. The design strength of this mix was specified as 27.6 MPa (4,000 psi). Two intermediate bents and two abutments support the superstructure (Figure 1a). The abutments and intermediate bent 2 were built with a concrete mixture using a 20% fly ash replacement of Portland cement with target compressive strength of 20.7 MPa (3,000 psi). Intermediate bent 3 was cast using HVFAC with a 50% fly ash

replacement of Portland cement designed with a specified compressive strength of 20.7 MPa (3,000 psi). As illustrated in Figure 1a, the bridge is skewed 30 degrees.

## 3 LIVE LOAD TEST PROGRAM

An automated total station (ATS) was used to record the girders deflection during a series of static load tests. A Leica TCA2003, which has an accuracy of 0.5 arc-seconds (angular measurements) and 1 mm + 1 ppm on distance measurements, was used. The first load test was conducted in April and August of 2014. Twenty four girder locations were selected to record the deflection of the superstructure. Fifteen ATS (prisms) were deployed along interior girder 3 at L/6, L/3, L/2, 2/3L and 5/6/L of each span. Three additional prisms were placed at midspan (L/2) of the remaining girders at each span (Figure 1a) MoDOT H20 dump trucks were employed to load the superstructure.

### 3.1 Load Test Configurations

Twelve load stops are reported herein. For load stops 1-3, two lane of trucks were driven from east towards west. The trucks were parked at the center of spans 3, 2 and 1, respectively (Figure 2a-c). For stops 4-6, the trucks were turned around, driven from west to east, and parked at the center of spans 1, 2, and 3, respectively. For these first 6 load stops, the center of the trucks' exterior axles was placed at 4.06 m (10.58 ft.) from the safety barrier's edge as illustrated in Figure 3a. For stops 7-9, the trucks were driven from west to east, but their exterior axles were separated 0.60 m (2 ft.) from the barrier's edge (Figure 3b). These first nine stops are identified as two-lane load cases. For stops 10-12 (Figure 2d-f), one lane of trucks was moved from west to east, and the truck were parked on the south side of the bridge, at 0.60 m (2 ft.) from the barrier's edge (only one lane of trucks in Figure 3b). The trucks were centered within the central region of each span as shown in Figure 2.

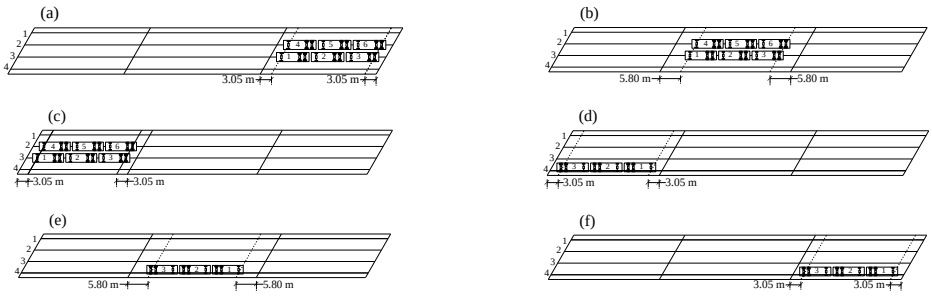


Figure 2. Load Test Configurations. (a) Stops 1, 6, and 9; (b) Stops 2, 5, and 8; (c) Stops 3, 4, and 7; (d) Stop 10; (e) Stop 11; (f) Stop 12.

### 3.2 Field Test Results

The vertical deflection values at midspan for the first 12 load stops are presented in Table 1. These deflection values correspond to the two-lane and one-lane load cases described on the previous section. Larger deflection values were obtained at midspan for the exterior and interior girders located in the vicinity of the applied load.

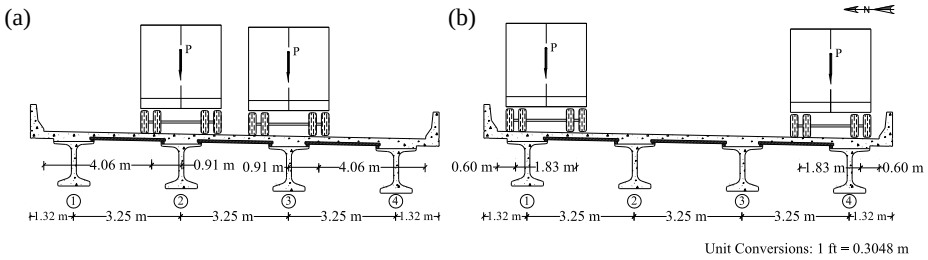


Figure 3. Distance from trucks' Exterior Axle to Barrier's Edge. (a) Stops 1-6; (b) Stops 7-12.

Table 1. Vertical deflections at midspan (two lanes loaded).

| Span | Stop | $\Delta_{G1}$ (mm) | $\Delta_{G2}$ (mm) | $\Delta_{G3}$ (mm) | $\Delta_{G4}$ (mm) |
|---|---|---|---|---|---|
| **Two Lanes Loaded** | | | | | |
| 1 | 3 | 5.1 | 6.9 | 6.7 | 4.9 |
| 1 | 4 | 4.2 | 6.7 | 6.9 | 4.4 |
| 1 | 7 | 4.9 | 5.1 | 5.5 | 5.7 |
| 2 | 2 | 6.3 | 9.7 | 9.5 | 6.2 |
| 2 | 5 | 6.4 | 9.8 | 10.1 | 6.4 |
| 2 | 8 | 7.3 | 7.8 | 8.1 | 7.6 |
| 3 | 1 | 4.2 | 7.1 | 6.9 | 4.6 |
| 3 | 6 | 4.9 | 8.4 | 7.8 | 5.2 |
| 3 | 9 | 4.4 | 5.5 | 5.9 | 5.9 |
| **One Lane Loaded** | | | | | |
| 1 | 10 | 0.102 | 1.270 | 3.531 | 5.004 |
| 2 | 11 | 0.762 | 1.981 | 4.928 | 7.747 |
| 3 | 12 | 1.219 | 2.108 | 3.531 | 5.410 |

Conversion factor: 25.4 mm = 1in.

## 4 LATERAL DISTRIBUTION FACTORS

The same nomenclature reported by Cai and Shahawy (2003) was employed. Thus, lateral distribution factors obtained from field measurements were defined as load distribution factors (LDF), and distribution factors obtained with the AASHTO LRFD (2012) equations were referred to as girder distribution factors (GDF).

### 4.1 Load Distribution Factors (LDF)

The LDF for interior and exterior girders presented in Table 2 were estimated from experimental deflections with Eq. (1).

$$LDF_i = \frac{\Delta G_i}{\sum_{i=1}^{n} \Delta G_i} \tag{1}$$

Where $LDF_i$ = load distribution factor of $i$th girder; $\Delta G_i$ = deflection of the $i$th girder at midspan; and $n$ = number of girders. The interior girders' LDF obtained for one-lane and two-lane load cases are similar to results reported by Pantelides et al. (2013) in the case of a bridge built with PC/PS AASHTO Type IV girders and precast deck panels reinforced with GFRP bars.

Table 2. Load Distribution Factors (Two Lanes Loaded).

| Span | Stop | $LDF_{G1}$ | $LDF_{G2}$ | $LDF_{G3}$ | $LDF_{G4}$ |
|---|---|---|---|---|---|
| **Two Lanes Loaded** | | | | | |
| 1 | 3 | 0.215 | 0.292 | 0.285 | 0.208 |
| 1 | 4 | 0.190 | 0.301 | 0.310 | 0.199 |
| 1 | 7 | 0.231 | 0.241 | 0.258 | 0.270 |
| 2 | 2 | 0.199 | 0.306 | 0.299 | 0.196 |
| 2 | 5 | 0.195 | 0.299 | 0.309 | 0.196 |
| 2 | 8 | 0.237 | 0.253 | 0.262 | 0.248 |
| 3 | 1 | 0.185 | 0.311 | 0.303 | 0.201 |
| 3 | 6 | 0.186 | **0.320** | 0.296 | 0.198 |
| 3 | 9 | 0.203 | 0.253 | 0.272 | **0.271** |
| **One Lane Loaded** | | | | | |
| 1 | 10 | 0.010 | 0.128 | **0.356** | **0.505** |
| 2 | 11 | 0.049 | 0.129 | 0.320 | 0.502 |
| 3 | 12 | 0.099 | 0.172 | 0.288 | 0.441 |

## 4.2 Girder Distribution Factors (GDF)

The AASHTO equations used to compute the flexural GDF and skew correction factors are presented in Table 3. Where $S$ = girder spacing (mm); $L$ = span length (mm); $t_s$ = deck thickness (mm); $K_g$ = stiffness parameter ($mm^4$); $n$ = modular ratio; $I_g$ = girder moment of inertia ($mm^4$); $e_g$ = girder eccentricity; $A_g$ = girder area ($mm^2$); $d_e$ = distance from exterior girder's centroid to barrier's edge (mm); $\theta$, skew angle; $SF$, skew correction factor (used if $30^o \leq \theta \leq 60^o$). The GDF values computed for interior and exterior girders are presented in Table 4. A multiple presence factor of 1.2 was employed to compute the exterior girders' GDF subject to one-lane loads. The lever rule approach was employed in such calculations.

Table 3. AASHTO LRFD Flexural GDF and Skew Correction Factor Equations.

| Interior | Exterior | |
|---|---|---|
| **Two or More Design Lanes Loaded** | | **Skew Factor** |
| $GDF_{int}^{m} = 0.075 + \left(\frac{S}{2900}\right)^{0.4}\left(\frac{S}{L}\right)^{0.2}\left(\frac{K_g}{Lt_s^{\,3}}\right)^{0.1}$ | $GDF_{ext}^{m} = \mathrm{e}\left(GDF_{int}^{m}\right)$<br>$\mathrm{e} = 0.77 + \frac{d_e}{2800} \geq 1$ | $SF = 1 - C_1(\tan\theta)^{1.5}$<br>$C_1 = 0.25\left(\frac{K_g}{Lt_s^{\,3}}\right)^{0.25}\left(\frac{S}{L}\right)^{0.5}$ |
| **One Design Lane Loaded** | | |
| $GDF_{int}^{s} = 0.06 + \left(\frac{S}{4300}\right)^{0.4}\left(\frac{S}{L}\right)^{0.3}\left(\frac{K_g}{Lt_s^{\,3}}\right)^{0.1}$ | $GDF_{ext}^{s} = m_p\left(\frac{S + d_e - 1524}{S}\right)$<br>Lever rule | |

## 5 RESULTS AND DISCUSSION

By definition, the values of LDF and GDF correspond to the maximum value of the interior and exterior girder that will produce a maximum load effect on the girders. As reported in Table 4, the value of the interior load distribution factor, $LDF_{int}$, and exterior load distribution factor, $LDF_{ext}$, were 0.505 and 0.356, respectively. The computed

interior girder distribution factor, $GDF_{int}$, was 0.783, and the exterior girder distribution factor, $GDF_{ext}$, was 0.936. The AASHTO GDF values were found to be larger and more conservative than the LDF computed from field measurements.

Table 4. Computed GDF (AASHTO LRFD).

| Span | Case | $GDF_{int}$ | $GDF_{int}$ (Corrected) | $GDF_{ext}$ | $GDF_{ext}$ (Corrected) |
|---|---|---|---|---|---|
| 1=3 | 2 or more lanes loaded | 0.819 | **0.783** | 0.901 | 0.861 |
| 1=3 | 1 lane loaded | 0.558 | 0.533 | 0.975 | 0.932 |
| 2 | 2 or more lanes loaded | 0.788 | 0.756 | 0.866 | 0.832 |
| 2 | 1 lane loaded | 0.528 | 0.507 | 0.975 | **0.936** |

## 6 PRELIMINARY CONCLUSIONS

The first full-scale structure implementation of high-strength self-consolidating concrete (HS-SCC) and high volume fly ash concrete (HVFAC) has been implemented on the structure of Bridge A7957 through the Missouri Department of Transportation.

The first series of live load tests was undertaken to establish a structure's response benchmark that will be used to monitor any change in the structure's response and to help validate design assumptions. Load distribution factors (LDF) were computed from field test measurements, and girder distribution factors (GDF) were estimated using the AASHTO LRFD approach. The GDF values were found to be conservative when compared to the LDF.

**Acknowledgments**

The authors gratefully acknowledge the financial support provided by the Missouri Department of Transportation (MoDOT) and the National University Transportation Center (NUTC) at Missouri University of Science and Technology.

## References

American Association of State Highway and Transportation Officials. "AASHTO LRFD Bridge Design Specifications, 6th Edition." *American Association of State Highway and Transportation Officials*. Washington (DC), 2012.

Barker, R.M., and Pucket, J.A., *Design of Highway Bridges: An LRFD Approach. 3rd Edition*. John Wiley & Son. Hoboken, New Jersey, 2013.

Cai, C.S., and Shahawy, M., Understanding Capacity Rating of Bridges from Load Tests. *ASCE Practice Periodical on Structural Design and Construction. 8(4), 209-216.* November, 2003.

Hernandez, E.S., Griffin, A., and Myers, J.J., Balancing Extended Service Life and Sustainable Concrete Usage in Missouri Bridge A7957, *2014 Structural Faults & Repair: European Bridge Conference (SF&R 2014)*, 9 pages, London, England, UK, July 8-10, 2014.

Myers, J.J., Volz, J.S., Sells, E., Porterfield, K., Looney, T., Tucker, B., and Holman, K., "Self-Consolidating Concrete (SCC) for Infrastructure Elements: Report A – Shear Characteristics," Final Report A MoDOT TRyy1103, Missouri Department of Transportation, Jefferson City, Missouri, August, 237 pp, 2012.

Pantelides, C.P., Ries, J., and Mix, R., Construction and Monitoring of a Single-Span Bridge with Precast Concrete Glass-Fiber-Reinforced Polymer Deck Panels. *PCI Journal, 58(1), 78-94.* Winter 2013.